Supporting Information

Hybrid 3D Nanostructures Based Hole Transport Layer for Highly Efficient Inverted Perovskite Solar Cells

Dan Ouyang[a], Cong Chen[b], Zhanfeng Huang[a], Lu Zhu[a], Yanfa Yan[b], Wallace C. H. Choy*[a]

[a] *Dr. Dan Ouyang, Dr. Zhanfeng Huang, Dr. Lu Zhu, Prof. Wallace C. H. Choy*
Department of Electrical and Electronic Engineering, The University of Hong Kong, Pokfulam Road, Hong Kong 999077, China
[b] *Mr. Cong Chen, Prof. Yanfa Yan*
Department of Physics and Astronomy, and Wright Center for Photovoltaics Innovation and Commercialization (PVIC), University of Toledo, Toledo, OH 43606, USA

E-mail: chchoy@eee.hku.hk

Keywords: Metal oxides, Nanostructure, Hole transport layer, Alignment band structure, Perovskite solar cells

Table S1. The average diameter and thickness of Cr:$CuGaO_2$-CC nanocrystals with different Cr doping concentrations.

Cr doping content	Average diameter (nm)	Thickness (nm)
1%	63±5.00	8±2.05
5%	39±4.56	8±1.94
7%	32±3.95	10±4.39

Table S2. The champion photovoltaic performance based on NiO_x and Cr:$CuGaO_2$-CC/NiO_x based PSCs.

HTL	Scan direction	J_{SC} (mA/cm^{-2})	V_{OC} (V)	FF	Best PCE (%)	Average PCE(%)
Cr:$CuGaO_2$-CC/NiO_x	Forward	22.93	1.08	0.80	19.91	18.26± 0.78
	Reverse	22.67	1.08	0.80	19.49	
Cr:$CuGaO_2$-CC	Forward	21.06	1.02	0.70	14.96	12.00± 0.91
	Reverse	19.60	1.01	0.68	13.46	
NiO_x	Forward	22.02	1.08	0.75	17.91	16.73± 0.60
	Reverse	21.45	1.07	0.73	16.75	

Table S3. Performance of the reported planar inverted PSCs based on 2D HTLs.

Device Architecture	V_{oc} (V)	J_{sc} (mA cm^{-2})	FF	PCE (%)	Method	Ref.
ITO/PEDOT:PSS+GO/$MAPbI_3$/PCBM/ZnO/Ag	1.02	21.55	0.82	18.09	wet chemical	[1]
ITO/PEDOT:PSS+GO+Glucose/$MAPbI_3$/PCBM/Ag	1.05	20.50	0.70	12.80	wet chemical	[2]
ITO/PEDOT:PSS+AgOTf doped GO/$MAPbI_3$/PCBM/Ag	0.88	19.18	0.71	11.90	CVD	[3]
ITO/MoO_x+GO/$MAPbI_3$/PCBM/Ag	0.99	21.80	0.77	16.70	wet chemical	[4]
ITO/NGGO/$MAPbI_3$/ZnO/Al	1.00	17.93	0.72	12.94	wet chemical	[5]
ITO/PEDOT:PSS/GO:NH_3/$MAPbI_3$/PCBM/Ag	1.03	22.06	0.71	16.11	wet chemical	[6]
ITO/PEDOT:PSS/oxo-G1/$MAPbI_3$/ZnO/Al	1.08	18.06	0.78	15.20	wet chemical	[7]
ITO/r-Go/PTAA/$MAPbI_3$/PCBM/BCP/Ag	1.09	20.30	0.78	17.20	wet chemical	[8]
ITO/MoS_2/$MAPbI_3$/PCBM/Li/Ag	0.96	14.89	0.67	9.53	Liquid exfoilated	[9]
ITO/MoS_2/$MAPbI_3$/PCBM/Ag	0.84	12.60	0.57	6.01	UVO	[10]
ITO/MoS_2/$MAPbI_3$/PCBM/BCP/Ag	0.88	20.94	0.78	14.35	Liquid exfoilated	[11]
ITO/WS_2/$MAPbI_3$/C_{60}/BCP/Ag	0.97	21.22	0.73	15.00	Liquid exfoilated	[11]
ITO/PEDOT:PSS/BPQDs/$MAPbI_3$/PCBM/Ag	1.01	20.13	0.80	16.69	Liquid exfoilated	[12]
ITO/PTAA/MoS_2/$MAPbI_3$/PCBM/PFN/Ag	1.01	20.71	0.78	16.42	Liquid exfoilated	[13]
ITO/MoS_2/$MAPbI_3$/TiO_2/Ag	0.93	26.25	0.84	20.43	Liquid exfoilated	[14]
ITO/Cr:$CuGaO_2$-cc/NiO_x/$MAPbI_{3-x}Cl_x$/PCBM:C_{60}/Zracac/Ag	**1.08**	**22.93**	**0.81**	**19.91**	**NPs in solution**	**this work**

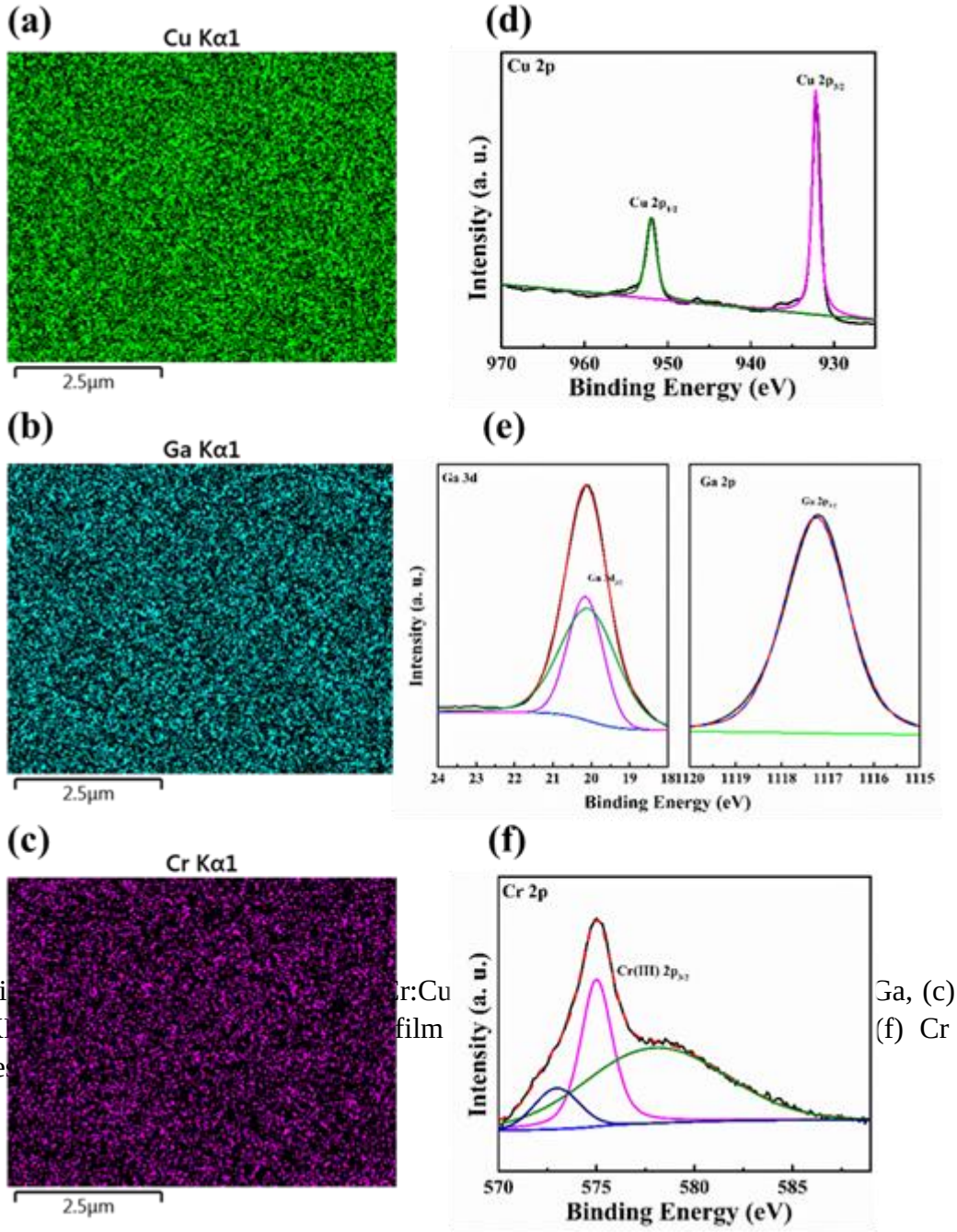

Fi r:Cu Ga, (c) Cr. X film (f) Cr 2p, re

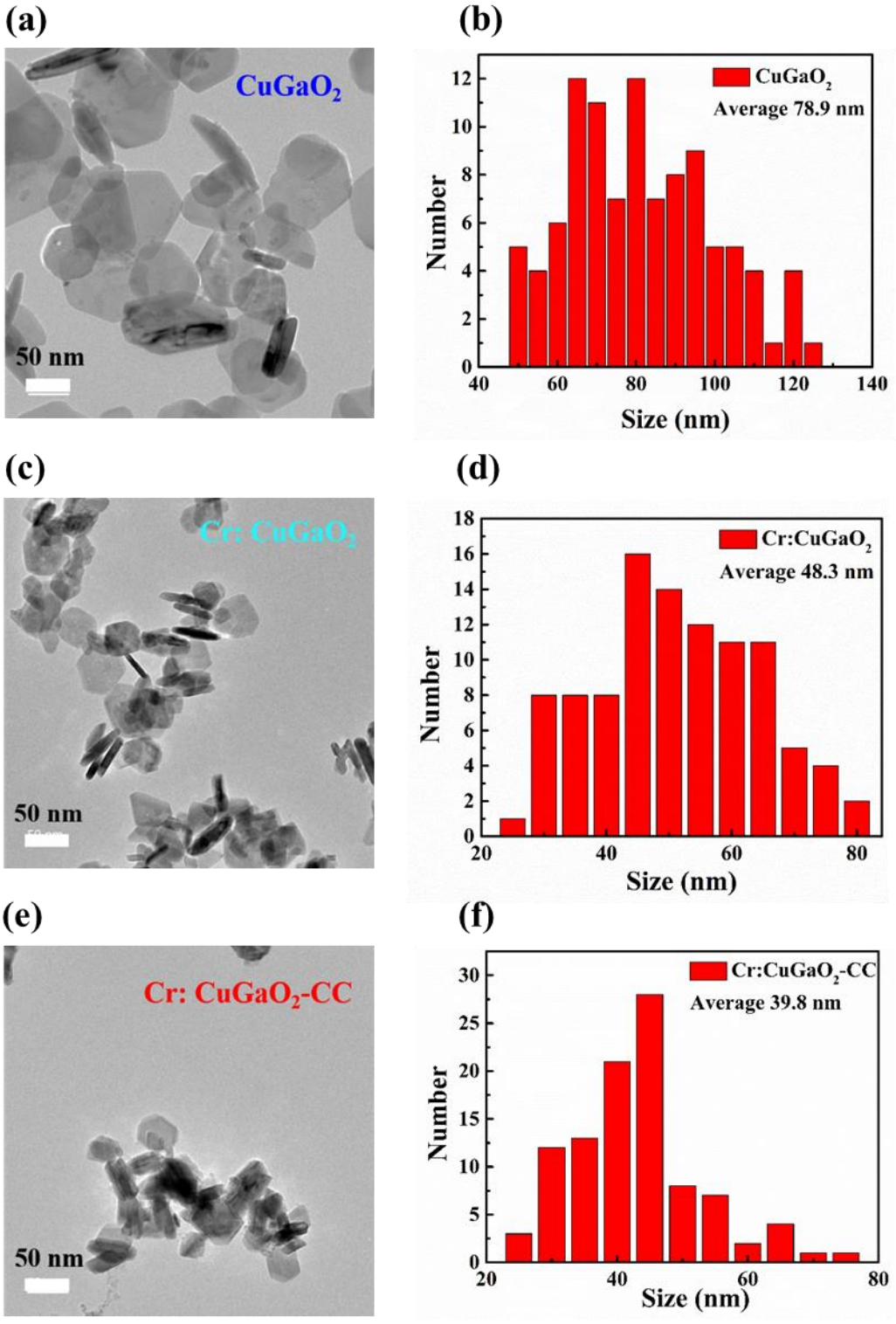

Figure S2. TEM images of (a) $CuGaO_2$, (c) $Cr:CuGaO_2$, and (e) $Cr:CuGaO_2$-CC nanocrystals. The size distribution of (b) $CuGaO_2$, (d) $Cr:CuGaO_2$, and (f) $Cr:CuGaO_2$-CC nanocrystals.

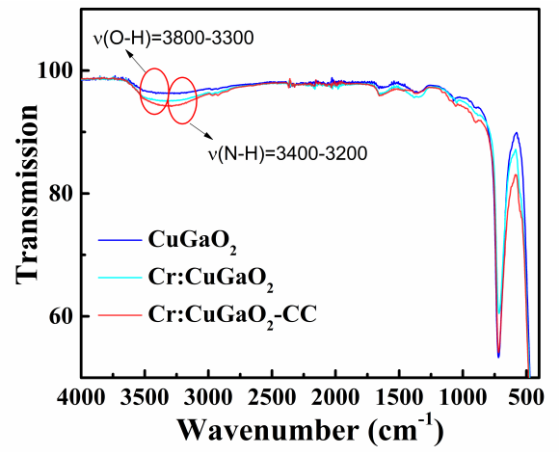

Figure S3. FTIR spectra of as-synthesized of $CuGaO_2$, $Cr:CuGaO_2$, and $Cr:CuGaO_2$-CC nanocrystals.

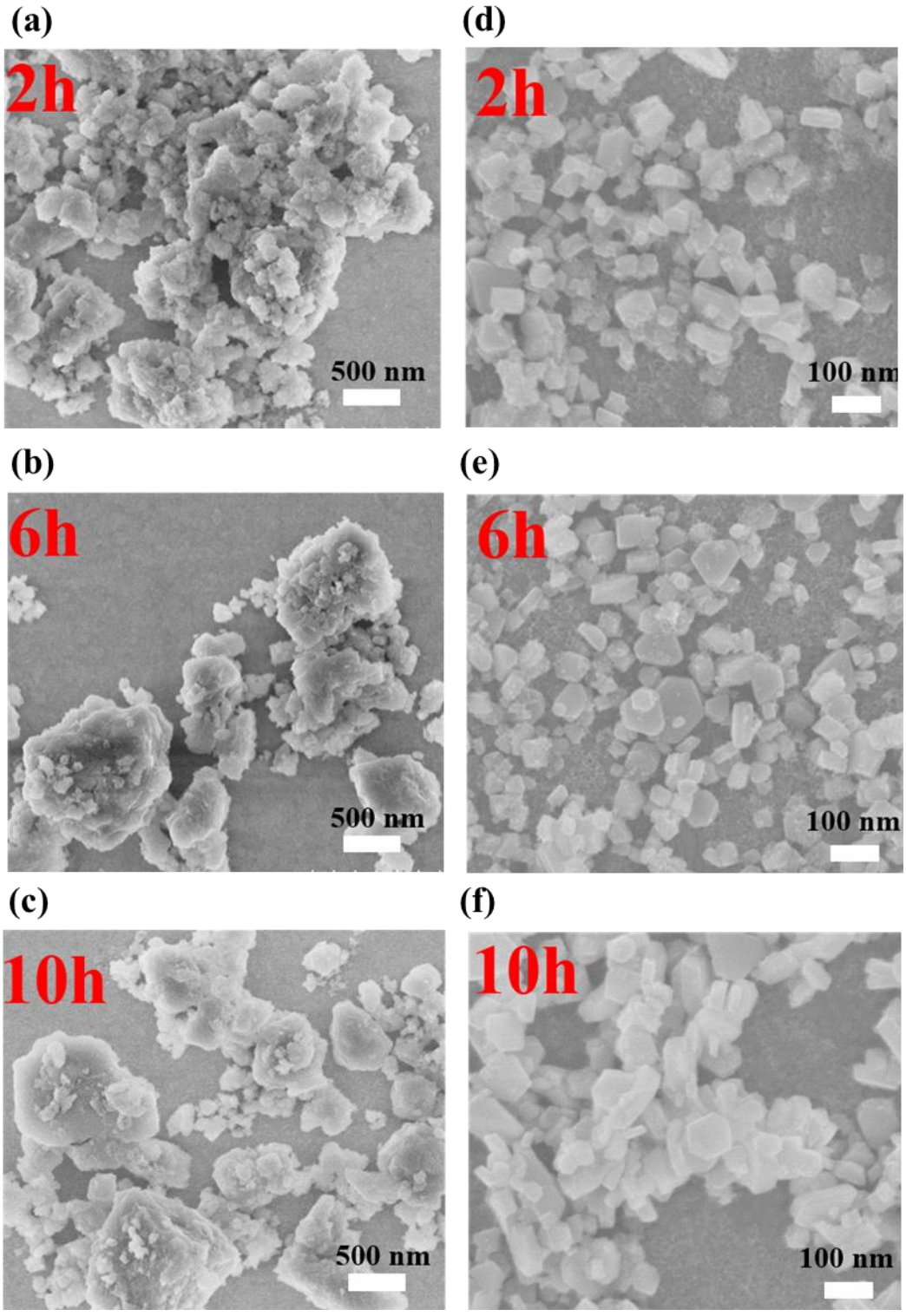

Figure S4. SEM images of the precursor before hydrothermal treatment under (a) 2h, (b) 6h, and (c) 10h aging time and the final Cr:$CuGaO_2$-CC nanocrystals under (d) 2h, (e) 6h, and (f) 10h aging.

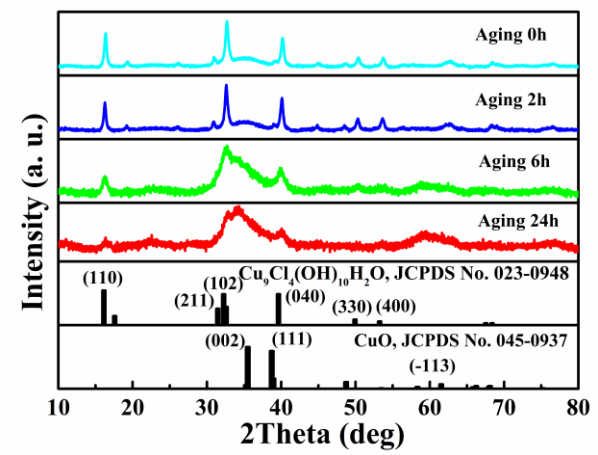

Figure S5. XRD patterns of the precursor before hydrothermal treatment at different aging times.

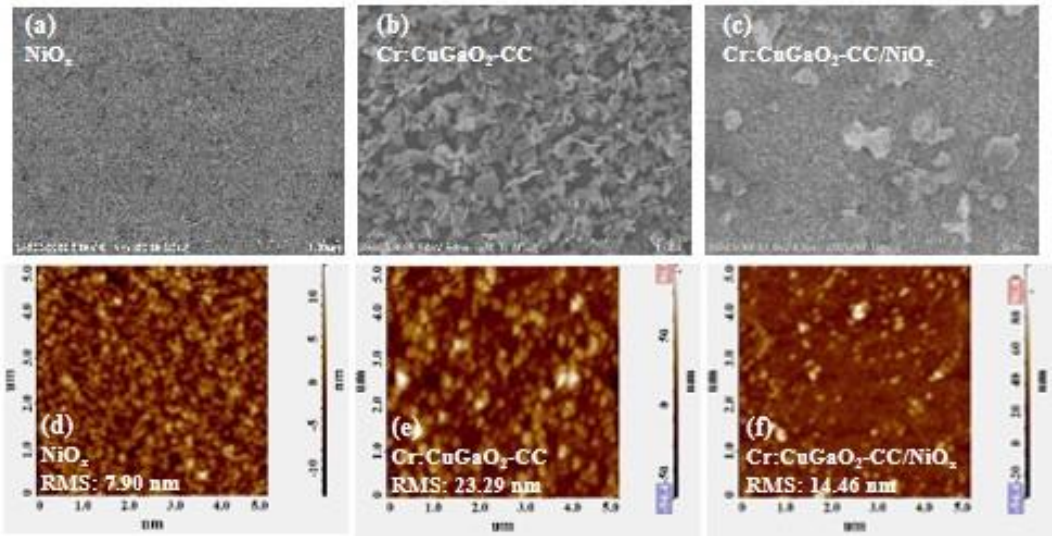

Figure S6. SEM (a) NiO_x, (b) $Cr:CuGaO_2$-CC, and (c) $Cr:CuGaO_2$-CC/NiO_x hybrid film, respectively. AFM image of (d) NiO_x, (e) $Cr:CuGaO_2$-CC, and (f) $Cr:CuGaO_2$-CC/NiO_x hybrid film, respectively.

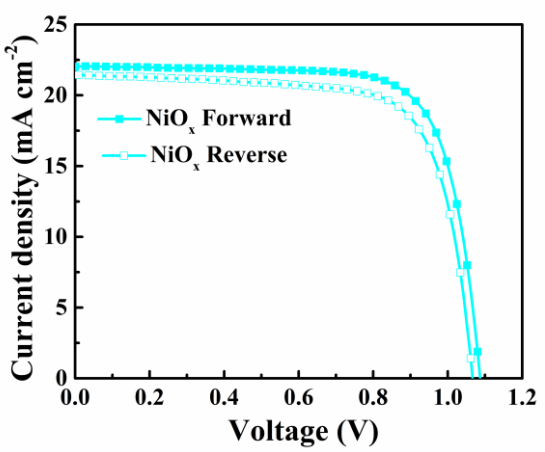

Figure S7. *J-V* characteristics of devices extracted from forward and reverse sweeping based on NiO_x HTL.

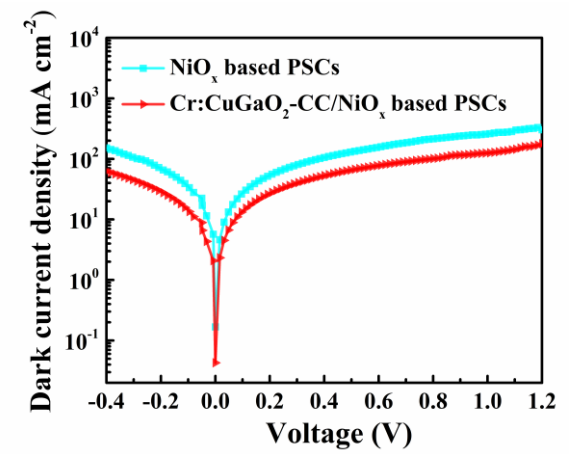

Figure S8. Dark current curves of the devices with NiO_x and Cr:$CuGaO_2$-CC/NiO_x HTL, respectively.

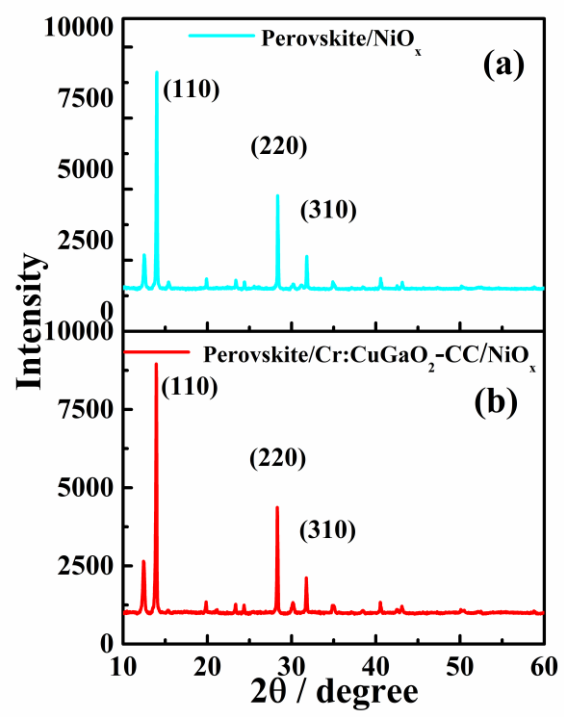

Figure S9. XRD patterns of perovskite crystals growth on (a) NiO_x and (b) $Cr:CuGaO_2$-CC/NiO_x HTL, respectively.

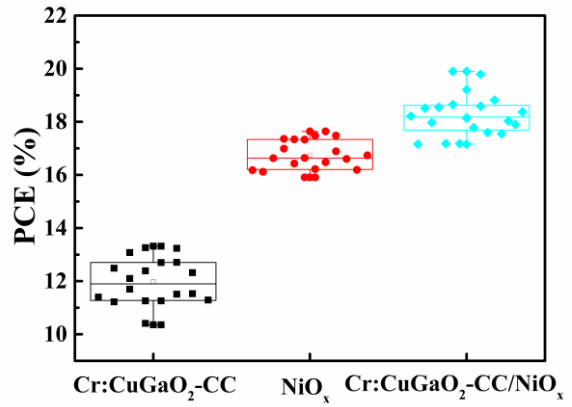

Figure S10. PCE histogram of 20 pristine Cr:$CuGaO_2$-CC, NiO_x and Cr:$CuGaO_2$-CC/NiO_x HTL based PSC devices.

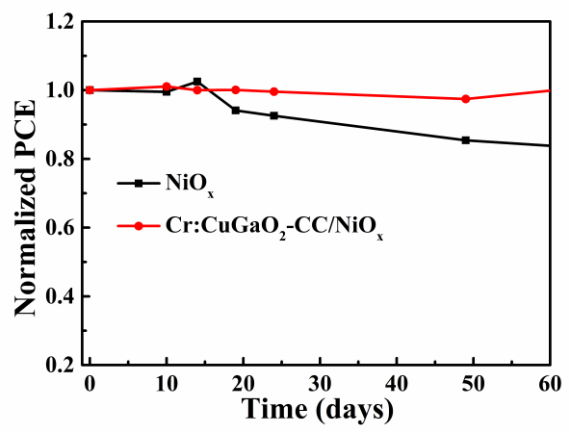

Figure S11. The storage stability of PSCs based on NiO_x and $Cr:CuGaO_2$-CC/NiO_x HTL.

Reference:

1. Yu, J. C.; Hong, J. A.; Jung, E. D.; Kim, D. B.; Baek, S.-M.; Lee, S.; Cho, S.; Park, S. S.; Choi, K. J.; Song, M. H. Highly Efficient and Stable Inverted Perovskite Solar Cell Employing PEDOT:GO Composite Layer as A Hole Transport Layer. *Sci Rep* **2018,** *8* (1), 1070, DOI: 10.1038/s41598-018-19612-7.

2. Guo, H.; Huang, X.; Pu, B.; Yang, J.; Chen, H.; Zhou, Y.; Yang, J.; Li, Y.; Wang, Z.; Niu, X. Efficiency Enhancement in Inverted Planar Perovskite Solar Cells by Synergetic Effect of Sulfated Graphene Oxide (sGO) and PEDOT:PSS as Hole Transporting Layer. *RSC Adv* **2017,** *7* (79), 50410-50419, DOI: 10.1039/c7ra10113a.

3. Liu, T.; Kim, D.; Han, H.; Mohd Yusoff, A. R. b.; Jang, J. Fine-tuning Optical and Electronic Properties of Graphene Oxide for Highly Efficient Perovskite Solar Cells. *Nanoscale* **2015,** *7* (24), 10708-10718, DOI: 10.1039/c5nr01433f.

4. Bhosale, S. S.; Jokar, E.; Fathi, A.; Tsai, C.-M.; Wang, C.-Y.; Diau, E. W.-G. Functionalization of Graphene Oxide Films with Au and MoOx Nanoparticles as Efficient p-Contact Electrodes for Inverted Planar Perovskite Solar Cells. *Adv Funct Mater* **2018,** *28* (37), 1803200, DOI: 10.1002/adfm.201803200.

5. Kim, J.; Mat Teridi, M. A.; Mohd Yusoff, A. R. b.; Jang, J. Stable and Null Current Hysteresis Perovskite Solar Cells based Nitrogen Doped Graphene Oxide Nanoribbons Hole Transport Layer. *Sci Rep* **2016,** *6* (1), 27773, DOI: 10.1038/srep27773.

6. Feng, S.; Yang, Y.; Li, M.; Wang, J.; Cheng, Z.; Li, J.; Ji, G.; Yin, G.; Song, F.; Wang, Z.; Li, J.; Gao, X. High-Performance Perovskite Solar Cells Engineered by an Ammonia Modified Graphene Oxide Interfacial Layer. *ACS Appl Mater Interfaces* **2016,** *8* (23), 14503-14512, DOI: 10.1021/acsami.6b02064.

7. Chen, H.; Hou, Y.; Halbig, C. E.; Chen, S.; Zhang, H.; Li, N.; Guo, F.; Tang, X.; Gasparini, N.; Levchuk, I.; Kahmann, S.; Ramirez Quiroz, C. O.; Osvet, A.; Eigler, S.; Brabec, C. J. Extending the Environmental Lifetime of Unpackaged Perovskite Solar Cells through Interfacial Design. *J Mater Chem A* **2016,** *4* (30), 11604-11610, DOI: 10.1039/c6ta03755k.

8. Zhou, Z.; Li, X.; Cai, M.; Xie, F.; Wu, Y.; Lan, Z.; Yang, X.; Qiang, Y.; Islam, A.; Han, L. Stable Inverted Planar Perovskite Solar Cells with Low-Temperature-Processed Hole-Transport Bilayer. *Adv Energy Mater* **2017,** *7* (22), 1700763, DOI: 10.1002/aenm.201700763.

9. Kim, Y. G.; Kwon, K. C.; Le, Q. V.; Hong, K.; Jang, H. W.; Kim, S. Y. Atomically Thin Two-dimensional Materials as Hole Extraction Layers in Organolead Halide Perovskite Photovoltaic Cells. *J Power Sources* **2016,** *319*, 1-8, DOI: 10.1016/j.jpowsour.2016.04.032.

10. Dasgupta, U.; Chatterjee, S.; Pal, A. J. Thin-film Formation of 2D MoS2 and Its Application as A Hole-transport Layer in Planar Perovskite Solar Cells. *Sol Energy Mater Sol Cells* **2017,** *172*, 353-360, DOI: 10.1016/j.solmat.2017.08.012.

11. Huang, P.; Wang, Z.; Liu, Y.; Zhang, K.; Yuan, L.; Zhou, Y.; Song, B.; Li, Y. Water-Soluble 2D Transition Metal Dichalcogenides as the Hole-Transport Layer for Highly Efficient and Stable p–i–n Perovskite Solar Cells. *ACS Appl Mater Interfaces* **2017,** *9* (30), 25323-25331, DOI: 10.1021/acsami.7b06403.

12. Chen, W.; Li, K.; Wang, Y.; Feng, X.; Liao, Z.; Su, Q.; Lin, X.; He, Z. Black Phosphorus Quantum Dots for Hole Extraction of Typical Planar Hybrid Perovskite Solar Cells. *J Phys Chem Lett* **2017,** *8* (3), 591-598, DOI: 10.1021/acs.jpclett.6b02843.

13. Kakavelakis, G.; Paradisanos, I.; Paci, B.; Generosi, A.; Papachatzakis, M.; Maksudov, T.; Najafi, L.; Del Rio Castillo, A. E.; Kioseoglou, G.; Stratakis, E.; Bonaccorso, F.; Kymakis, E. Extending the Continuous Operating Lifetime of Perovskite Solar Cells with a Molybdenum Disulfide Hole Extraction Interlayer. *Adv Energy Mater* **2018,** *8* (12), 1702287, DOI: 10.1002/aenm.201702287.

14. Kohnehpoushi, S.; Nazari, P.; Nejand, B. A.; Eskandari, M. MoS2: A Two-dimensional Hole-transporting Material for High-efficiency, Low-cost Perovskite Solar Cells. *Nanotechnology* **2018,** *29* (20), 205201, DOI: 10.1088/1361-6528/aab1d4.